MATERIALS AND INTERFACES

Mechanisms for the Removal of Calcium Phosphate Deposits in Turbulent Flow

Felicia Littlejohn† and Christine S. Grant*

Department of Chemical Engineering, North Carolina State University, Raleigh, North Carolina 27695-7905

A. Eduardo Sáez

Department of Chemical and Environmental Engineering, University of Arizona, Tucson, Arizona 85721

This work investigates the mechanisms for the removal of calcium phosphate deposits from stainless steel tubing in turbulent flows. Two types of deposits were analyzed: brushite (dicalcium phosphate dihydrate, DCPD) and a mixture of DCPD/hydroxyapatite (HAP). Cleaning studies were carried out at pHs ranging from 2.85 to 10. The data were analyzed by means of a mathematical model that incorporates the effects of interfacial dissolution and mass transfer. The results show that the HAP/DCPD cleaning rate is influenced both by the kinetics of the interfacial dissolution and by mass transfer. Within the same range of experimental conditions, the rate-limiting mechanism for DCPD removal was the abrasion of the solid by shear stresses. In this case, the interfacial dissolution process plays the role of decreasing the structural integrity of the deposit. These findings show that the removal mechanism of the HAP/DCPD mixture differs significantly from the behavior of individual components.

Introduction

The precipitation of hardness salts results in the formation of mineral deposits that are difficult to clean. The composition of mineral scales varies depending on the composition of hardness salts in solution. In general, these scales may consist of carbonates, sulfates, phosphates, and silicates. The formation of calcium phosphate scales has become more predominant in some applications because of (1) the replacement of toxic chromate compounds with phosphate compounds to curb corrosion and (2) the processing of recycled or untreated water containing high phosphate concentrations.[1,2]

Typically, calcium phosphate deposits consist of a mixture of different solid phases. In heat-exchanger systems, the calcium phosphate scales are characteristic of hydroxyapatite (HAP; $Ca_5(PO_4)_3OH$).[1] In cooling towers, a precursor to HAP, amorphous calcium phosphate (ACP), initially forms. Similarly, the mineral components of milk fouling deposits formed at high temperatures (T > 130 °C) consist primarily of calcium phosphate. The most common mineral components in these milk fouling deposits appear to be HAP, brushite or dicalcium phosphate dihydrate (DCPD; $CaHPO_4 \cdot 2H_2O$), and octacalcium phosphates (OCP; $Ca_8H_2(PO_4)_6 \cdot 5H_2O$).[3] Dental calculi have been characterized as consisting of carbonated HAP, DCPD, OCP, and tricalcium phosphate (TCP; $Ca_3(PO_4)_2$).[4]

Because of the complexity of mineral deposits, understanding the cleaning characteristics of calcium phosphate mixtures is of practical importance. This research studies the removal of deposits consisting of HAP and DCPD. Hydroxyapatite is traditionally studied as a model calcium phosphate, because it is the most thermodynamically stable form of calcium phosphate under most conditions. The structure of HAP consists of calcium and orthophosphate (PO_4^{3-}) tetrahedra arranged in columns parallel to the hexagonal axis.[5]

While HAP has been studied extensively, DCPD has received much less attention. Brushite is important in the study of calcium phosphate deposit removal, because it tends to precipitate and dissolve more readily than anhydrous salts under most conditions.[6] The precipitation and solubilization properties are influenced by the crystal structure. Brushite consists of parallel sheets of $CaHPO_4$ linked by water molecules.[7] Hydrated ions are readily incorporated into the hydrated crystal resulting in crystal growth[7] or, likely, dissolution.

In previous works, our group studied the removal of calcium phosphate deposits from stainless steel pipes under turbulent flow conditions using an on-line solid scintillation technique. This technique involves the use of ^{32}P-labeled deposits in an experimental flow system equipped with solid scintillation detection equipment. Grant et al.[8] prepared calcium phosphate deposits by precipitation from solution and measured removal rates under strongly acidic conditions (pHs below 3.5). On the basis of measured Ca/P ratios, Grant et al. inferred that the deposits were a mixture of DCPD and HAP but, in principle, other calcium salts could have been present in the precipitated solids. The effect of fluid flow on the cleaning rates suggested that mass transfer plays a significant role in the removal of calcium phosphate. In

* To whom correspondence should be addressed. E-mail: grant@eos.ncsu.edu. Telephone: 919-515-2317. Fax: 919-515-3465.

† Current address: E.I. duPont de Nemours and Co., Chattanooga, TN.

10.1021/ie990624h CCC: $19.00
Published on Web 03/10/2000

a recent work, we studied the removal of HAP/DCPD deposits using solutions of the sequestering agent sodium polyaspartate.[9]

The acid dissolution of calcium minerals is often studied by means of batch dissolution experiments, in which the dissolution rate of suspended solids in a stirred reservoir is monitored as a function of time. In a series of papers, Christoffersen and co-workers[10−12] studied the acid dissolution of HAP in batch dissolution experiments. They established that the dissolution process at the interface between the solid and the liquid imposed kinetic limitations. Thomann et al.[13−16] also conducted batch dissolution experiments with HAP, reaching similar conclusions. Batch dissolution experiments were also performed with DCPD.[17−21] The solubility of DCPD at moderate and high pHs is substantially higher than other calcium minerals, and solutions of practical relevance, such as cleaning solutions, tend to be undersaturated with respect to DCPD. The dissolution of DCPD powder is controlled primarily by volume diffusion at high degrees of undersaturation.[18] Altering the degree of undersaturation affects the dissolution mechanism. Decreasing the relative undersaturation of the solution (and hence the driving force for dissolution) resulted in an increase in the pH at which the minimum dissolution rate occurred.[21] At a relatively low degree of undersaturation, the dissolution rate is controlled by interfacial processes, such as the rate of ion detachment and surface diffusion processes.[20]

Even though they provide information on dissolution rates, batch dissolution experiments are not convenient when mass transfer plays a role. For the typical case of polydisperse, nonspherical solid particles suspended in a fluid by constant stirring, whose shape and size change with time, estimation of the mass-transfer coefficient is difficult.

A technique commonly employed to examine the relative importance of mass-transfer and interfacial processes in dissolution is the rotating disk method.[22−24] This technique involves the affixation of the solid of interest on a disk. This disk is attached to a shaft that is rotated at the desired speed. The well-defined hydrodynamics of the rotating disk method enables a quantitative determination of the mass-transfer rates.

A channel flow method, developed by Compton et al.,[25] applies an electrochemical detection technique to measure the interfacial properties of a carbonate crystal directly under well-characterized laminar flow conditions. This technique involves the attachment of a crystal to one wall of a rectangular duct. Then, as fluid flows through the duct, an electrode positioned adjacent to and downstream of the crystal takes measurements that correspond to the flux (or concentration) distribution of the species at the crystal/solution interface. This technique is particularly well suited for the study of interfacial processes during mineral dissolution.

In this work, we use a solid scintillation technique to study removal of DCPD and HAP/DCPD deposits from stainless steel pipes under turbulent flow conditions. The main objective is to determine the mechanisms by which the deposits are removed at various pHs and fluid velocities. By comparing pure DCPD deposits to HAP/DCPD mixtures, we will establish how the deposit composition affects the cleaning rate and removal mechanism.

We postulate that, in general, deposit removal might be controlled by one or more of three distinct processes: (1) interfacial solubilization of the calcium mineral; (2) mass transfer from the solid surface to the bulk fluid; and (3) detachment of solids from the deposit because of the action of shear forces. Establishing which of the three mechanisms is the slow step under a given set of conditions will depend on removal rate data at various fluid velocities. In the next section, we summarize the analysis presented by Grant et al.[8] for the case in which mass transfer is the rate-limiting step.

Transport-Limited Dissolution. The molar flux of a solubilized chemical species from the solid/liquid interface to the bulk liquid is given by

$$J = k_m(C_i - C_b) \tag{1}$$

where C_i and C_b are the interfacial and bulk concentrations of the dissolved species, respectively, and k_m is the mass-transfer coefficient. For systems with well-defined fluid flow, such as flow in cylindrical tubes, empirical correlations have been developed to determine the value of the mass-transfer coefficient.

To devise quantitative cleaning models that include mass transfer, the concentration difference $(C_i - C_b)$ must be known. While the concentration of solubilized material in the bulk solution, C_b, may be measured, the interfacial concentration, C_i, is related to the interfacial dissolution rate and the solubility. The solubility, C_s, is determined by thermodynamic equilibria. A relatively fast dissolution rate results in the instantaneous attainment of equilibrium at the solid/liquid interface, i.e., $C_i = C_s$. This approach was applied by Grant et al.[8]

Consider the dissolution of a deposit from the inner wall of a pipe in turbulent flow. The differential mass of the deposit, dM, remaining on a portion dz of the pipe surface obeys the following mass balance:

$$\frac{\partial(\mathrm{d}M)}{\partial t} = -JM_w\,\mathrm{d}S = -k_m(C_i - C_b)M_w\pi D\,\mathrm{d}z \tag{2}$$

where dS is the surface area of the deposit, D is the diameter of the fluid cross section (which, for a thin deposit, is approximately equal to the internal pipe diameter), and M_w is the average molecular weight of the film. In Grant et al.'s experiments, $C_b \approx 0$ due to the high volume of cleaning solution relative to the initial mass of the deposit and the low solubility of calcium phosphate. The mass-transfer coefficient, k_m, can be represented by an empirical correlation of the form

$$Sh = \frac{k_m D}{D_A} = aRe^b Sc^c \tag{3}$$

where Sh is the Sherwood number, the Reynolds and Schmidt numbers are defined by $Re = \rho v_z D/\mu$, $Sc = \mu/\rho D_A$, v_z is the average fluid velocity, μ and ρ are the viscosity and the density of the bulk fluid, respectively, D_A is the diffusivity of the dissolving species in water, and a, b, and c are constants that depend on the flow regime. For turbulent flow in pipes, $a = 0.023$, $b = 0.83$, and $c = {}^1/_3$.[26]

After substitution of k_m in eq 2 and integration along the total length of the pipe covered by deposit, L, the following expression for the removal rate is obtained:

$$-\frac{\mathrm{d}M}{\mathrm{d}t} = \pi DLM_w C_i \frac{[aD^{b-1}\rho^{b-1}Sc^{c-1}]}{\mu^{b-1}} v_z{}^b \tag{4}$$

Table 1. Equilibrium Reactions Accounted for in the $Ca(OH)_2-H_3PO_4-H_2O$ System at 37 °C[7]

equilibrium reaction	equilibrium constant
calcium salt solubility	
$CaHPO_4 = Ca^{2+} + HPO_4^{2-}$	$k_{dcpd} = (Ca^{2+})(HPO_4^{2-}) = 2.37 \times 10^{-7}$ mol^2/L^2
$Ca_5(PO_4)_3OH = 5Ca^{2+} + 3\ PO_4^{3-} + OH^-$	$k_{hap} = (Ca^{2+})^5(PO_4^{3-})^3(OH^-) = 2.35 \times 10^{-59}$ mol^9/L^9
phosphate equilibria	
$H_3PO_4 = H^+ + H_2PO_4^-$	$k_1 = (H^+)(H_2PO_4^-)/(H_3PO_4) = 6.18 \times 10^{-3}$ mol/L
$H_2PO_4^- = H^+ + HPO_4^{2-}$	$k_2 = (H^+)(HPO_4^{2-})/(H_2PO_4^-) = 6.59 \times 10^{-8}$ mol/L
$HPO_4^{2-} = H^+ + PO_4^{3-}$	$k_3 = (H^+)(PO_4^-)/(HPO_4^{2-}) = 4.29 \times 10^{-13}$ mol/L
ion-pair formation	
$Ca^{2+} + HPO_4^{2-} = CaHPO_4^0$	$k_x = (CaHPO_4^0)/(Ca^{2+})(HPO_4^{2-}) = 681$ L/mol
$Ca^{2+} + H_2PO_4^- = CaH_2PO_4^+$	$k_y = (CaH_2PO_4^+)/(Ca^{2+})(HPO_4^-) = 31.9$ L/mol
$Ca^{2+} + OH^- = CaOH^+$	$k_4 = (CaOH^+)/(Ca^{2+})(OH^-) = 32.4$ L/mol
$Ca^{2+} = 2OH^- = Ca(OH)_2$	$k_5 = (Ca(OH)_2)/(Ca^{2+})(OH^-)^2 = 4.68 \times 10^{-6}$ L/mol
$Ca^{2+} + PO_4^{3-} = CaPO_4$	$k_6 = (CaPO_4^-)/(Ca^{2+})(PO_4^{3-}) = 2.9 \times 10^6$ L/mol
water equilibria	
$H_2O = H^+ + OH^-$	$k_w = (H^+)(OH^-) = 2.485 \times 10^{-14}$ mol^2/L^2

If the interfacial solubilization process is fast relative to mass transfer, then $C_i = C_s$, and eq 4 indicates that the removal rate, $-dM/dt$, would be directly proportional to the average velocity to the 0.83rd power. On the other hand, the dependence of the removal rate on pH in this case would be determined be the changes in solubility with pH. For low pHs (below 3.5) and using a deposit that consisted of a precipitated calcium phosphate, Grant et al.[8] found a velocity exponent of 0.70. Because this value is close to the 0.83 exponent predicted by the transport-limited model, they concluded that mass transfer was the slow step under the conditions studied.

The application of predictive mass-transfer models relies on a knowledge of the solubility of the deposit at the interface. In the following section, we will discuss the solubility of the calcium minerals used in this work.

Calcium Phosphate Solubility. Gregory et al.[27] and McDowell et al.[28] studied the solubility equilibria for systems containing $Ca(OH)_2-H_3PO_4-H_2O$ for DCPD and HAP, respectively. The equilibrium reactions are shown in Table 1. This system of equations consists of solubilization reactions, the formation of ion pairs, water equilibria, phosphate equilibria, and calcium hydrolysis. Note that neglecting the ion pairs, $CaHPO_4^0$ and $CaH_2PO_4^+$, results in the determination of apparent solubility products that vary with the equilibrium pH.[27] However, the concentrations of these ion pairs are usually insignificant, i.e., less than 10−20% of the total calcium or orthophosphate in solution.[6] Above pH 7 or 8, the concentration of the ion pair $CaPO_4^-$ may be significant.[6]

The equilibrium reactions (Table 1) may be solved to determine the ion activities of all species resulting from the solubilization process by applying the necessary constraints. Possible constraints are mass balances, congruent dissolution, saturation conditions at the crystal surface, and electroneutrality. Application of the electroneutrality constraint in some systems was found to adversely affect the solution of the equilibrium equations.[20] This result was attributed to a redundancy of the electroneutrality equation with the saturation conditions. Alternately, the condition of electroneutrality is necessary to calculate the pH[6] and hence should not be included if the pH is known.

For a given pH, the following constraints may be applied to DCPD and HAP:

$$\text{Ca balance: } [Ca] = [Ca^{2+}] + [CaHPO_4^0] + [CaH_2PO_4^+] + [CaOH^+] + [Ca(OH^+)_2] \quad (5)$$

$$\text{P balance: } [P] = [H_3PO_4] + [H_2PO_4^-] + [HPO_4^{2-}] + [PO_4^{3-}] \quad (6)$$

$$\text{Congruent dissolution of DCPD: } [Ca]/[P] = 1.000 \quad (7)$$

$$\text{Congruent dissolution of HAP: } [Ca]/[P] = 1.667 \quad (8)$$

Note that molar activities are represented by species in parentheses and concentrations are denoted by brackets. The activity, a_j, and concentration, C_j, of species j are related by

$$a_j = \gamma_j C_j \quad (9)$$

where γ_j is the activity coefficient of species j. The activity coefficient was calculated by the Davies expression[29]

$$-\log \gamma_j = A z_j^2 \frac{\sqrt{I}}{1+\sqrt{I}} - 0.3I \quad (10)$$

where A is a temperature-dependent constant given a value of 0.52 and at 37.5 °C,[27] z_j is the charge of species j, and I is the total ionic strength of the solution. The following equation was used to calculate the ionic strength:

$$I = \frac{1}{2}\sum [C_j] z_j^2 \quad (11)$$

The solution to the solubility equilibria (Table 1) and constraints (eqs 5−8 as appropriate) yield the solubility isotherms for HAP and DCPD shown in Figure 1.[7]

Theory

In this section, we will develop a theory to describe the removal rates of calcium phosphate deposits under turbulent flow conditions considering possible kinetic limitations due to interfacial dissolution and mass transfer. We will then discuss how mechanical removal of solids due to shear affects the derivation. The purpose of the presentation of the theory is to establish a basis for analyzing the experimental data.

The kinetics of the interfacial dissolution process will be modeled as a chemical reaction. To simplify the formulation of the theory, we will consider the dissolu-

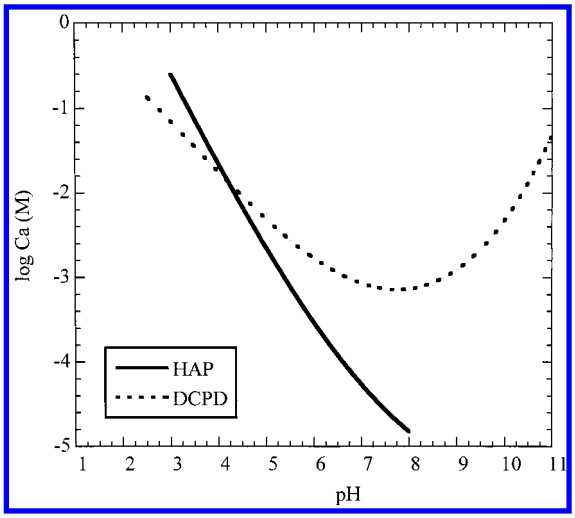

Figure 1. Solubility isotherms for calcium phosphate at 37 °C.[7,8]

tion of a deposit consisting only of DCPD. Later, the analysis will be generalized to address deposits composed of a HAP/DCPD mixture. Additionally, we will initially consider interfacial and mass-transfer processes only, neglecting the possible removal of the deposit by detachment of solids due to shear forces.

The dissolution of DCPD involves reactions at the solid/liquid interface and liquid-phase equilibrium processes. While the exact dissolution mechanism is unknown, the interfacial kinetics may be represented by assuming that the slow step is the solubilization of the calcium salt into the liquid phase. We will assume that the acid/base reactions and the ion-pair reactions (Table 1) achieve equilibrium instantaneously and that the interfacial dissolution mechanism is controlled by the rate of DCPD solubilization. The interfacial solubilization of DCPD in water is expressed as the following reversible reaction:

$$CaHPO_4{\cdot}H_2O(s) \rightleftharpoons Ca^{2+} + HPO_4^{2-} + H_2O \quad (12)$$

If this reaction follows an elementary rate law, the dissolution flux of DCPD is given by

$$J = k_1' - k_{-1}[Ca^{2+}]_i[HPO_4^{2-}]_i\gamma_{Ca^{2+}}\gamma_{HPO_4^{2-}} \quad (13)$$

The forward and reverse rate constants are represented by k_1' and k_{-1}, respectively.

Because the exact dissolution reactions are not known and the relevance of different reactions might change with changes in the conditions (e.g., pH), we will consider eq 13 as a general mathematical statement representing the net reaction that leads to the dissolution of the mineral. Depending on the elementary reactions that make up the dissolution mechanism, the rate constants in eq 13 are then allowed to vary with changes in the dissolution conditions. To illustrate this point, consider a mechanism in which proton attack induces the dissolution of the mineral,

$$CaHPO_4{\cdot}H_2O(s) + H^+ \rightleftharpoons Ca^{2+} + H_2PO_4^- + H_2O \quad (14)$$

The kinetics of this reaction can still be represented by eq 13, but this will lead to a forward rate constant, k_1', that is directly proportional to the concentration of protons.

Using eq 6 and the phosphate equilibria shown in Table 1, it can be shown that

$$[HPO_4^{2-}] = \alpha[P] \quad (15)$$

where α is only a function of pH and the ionic strength. Based on an assumption that the ion-pair concentrations (shown in eq 5) are negligible, eq 7 is rewritten as

$$[Ca^{2+}] = [P] \quad (16)$$

Combining eqs 13, 15, and 16, the following expression is obtained for the flux:

$$J = k_1'\left(1 - \frac{[Ca^{2+}]_i^2}{K_{Eq}}\right) \quad (17)$$

where $K_{Eq} = k_{dcpd}/(\alpha\gamma_{Ca^{2+}}\gamma_{HPO_4^{2-}})$ and where the definition $k_{dcpd} = k_1'/k_{-1}$ is applied.

At equilibrium, $[Ca^{2+}]_i = [Ca^{2+}]_s$ and the flux, J, approaches zero. With substitution of the equilibrium constraints into eq 17, $K_{Eq} = [Ca^{2+}]_s^2$. Therefore, the equation is rewritten as

$$J = k_1'\left(1 - \left(\frac{[Ca^{2+}]_i}{[Ca^{2+}]_s}\right)^2\right) \quad (18)$$

Equation 18 describes the flux of calcium from the crystal surface by solubilization of calcium phosphate.

Under pseudosteady state, the flux of calcium released by solubilization of calcium phosphate at the solid/liquid interface is equal to the flux of calcium transported from the solid/liquid interface to the bulk solution. As stated previously, the driving force for mass transfer is the concentration gradient (eq 2). Expressing eq 2 in terms of the calcium ion concentration, we obtain

$$J = k_m([Ca^{2+}]_i - [Ca^{2+}]_b) \quad (19)$$

Because cleaning processes are carried out in large quantities of dilute solutions, $[Ca^{2+}]_b \approx 0$.

Limiting Conditions for Removal by Calcium Phosphate Dissolution. The derivations incorporate both the effects of a reversible interfacial solubilization process and the effect of mass transfer on the removal rate. If one mechanism is rate controlling, eqs 18 and 19 may be simplified. Consider the case in which the rate of mass transfer is very fast ($k_m \rightarrow \infty$) so that the interfacial solubilization process is rate-limiting. In this case, all dissolved calcium is instantaneously transported to the bulk solution, i.e., $[Ca^{2+}]_i = 0$. Equation 18 reduces to

$$J = k_1' \quad (20)$$

Equation 20 shows that the flux is velocity independent.

By contrast, if the interfacial process is fast, the flux is mass-transfer-controlled. As noted previously, mass-transfer-limited mechanisms are based on the assumption that attainment of equilibrium at the solid/liquid interface is instantaneous, i.e., $[Ca^{2+}]_i = [Ca^{2+}]_s$. Thus, when eq 4 is rewritten in terms of Ca^{2+}

$$J = k_m[Ca^{2+}]_s = \frac{aD^{b-1}\rho^{b-1}Sc^{c-1}}{\mu^{b-1}}[Ca^{2+}]_s v_z^b \quad (21)$$

For mass-transfer-limited removal into turbulent streams flowing through pipes, the flux is proportional to $v_z^{0.83}$.

In summary, the velocity dependence provides a strong indication of the removal mechanisms. If we formulate a velocity dependence for the flux as

$$J = \kappa v_z^{\beta} \tag{22}$$

for dissolution processes controlled by the kinetics of the interfacial process, $\beta = 0$. If the process is controlled by the rate of mass transfer, then the velocity dependence of the flux is given by $\beta = b = 0.83$. If both mechanisms contribute significantly to the removal rate, then an intermediate velocity dependence should be attained, i.e., $0 < \beta < 0.83$.

An analysis similar to that presented above can be developed for HAP dissolution. Even though the interfacial dissolution mechanism will be undoubtedly different, the limiting cases will be subject to the same velocity dependence, so that a behavior represented by eq 22 should be obtained.

For a mixture HAP/DCPD, the behavior is potentially more complicated because of the different levels of solubility. However, in the turbulent flow experiments conducted in this work, the calcium concentration of the bulk liquid is approximately zero. This means that the dissolved calcium will be carried away by the liquid flow. On this basis, we postulate that the dissolution of the mixture can be envisioned as the dissolution of a surface that is partly composed of HAP and DCPD. In other words, we will consider dissolution as being independent for each mineral. The dissolution flux for the mixture, J_{HD}, can then be expressed as

$$J_{HD} = hJ_H + (1 - h)J_D \tag{23}$$

where J_H and J_D are the dissolution fluxes of HAP and DCPD, respectively, and h is the fraction of the surface occupied by HAP. Substituting eq 22 for each component yields

$$J_{HD} = h\kappa_H v_z^{\beta_H} + (1 - h)\kappa_D v_z^{\beta_D} \tag{24}$$

In the limiting case of fast mass transfer, $\beta_H = \beta_D = 0$, and for fast interfacial dissolution, $\beta_H = \beta_D = b = 0.83$, so that the dissolution flux of the mixture will follow a trend given by

$$J_{HD} = \kappa_{HD} v_z^{\beta_{HD}} \tag{25}$$

where $0 < \beta_{HD} < 0.83$.

We have shown that an analysis of the effect of the average velocity on dissolution rates can establish the relative importance of interfacial dissolution kinetics and mass transfer. Next, we extend the theory to deposit removal due to shear forces.

Limiting Conditions for Calcium Phosphate Removal by Shear Stresses. The rate-controlling mechanism for calcium phosphate removal may also be the mechanical removal of undissolved solids. Under turbulent flow conditions, the shear stress exerted on calcium phosphate by the fluid is given by

$$\tau_w = \frac{1}{8}\rho v_z^2 f \tag{26}$$

where τ_w is the shear stress exerted at the solid/liquid interface and f is the Darcy friction factor. For rough surfaces and sufficiently high Reynolds numbers, the friction factor is independent of the average velocity. In the case of a pipe covered by a calcium deposit, the surface is rougher than a typical commercial pipe, as shown by SEM micrographs presented by Littlejohn et al.[9] for HAP/DCPD mixtures. These deposits are composed of agglomerated HAP and DCPD crystals.

To remove the calcium phosphate, the turbulent shear forces exerted by the fluid must exceed the force per unit area that the agglomerated crystals can withstand intact, τ_c. The criterion for deposit removal by the shear forces exerted on the deposit by fluid flow can be written as

$$\tau_w \geq \tau_c \tag{27}$$

Thus, when mechanical removal by shear forces dominates, the removal rate is likely to be directly proportional to v_z^2. Thus, the role of shear-based removal may also be assessed by an examination of the velocity dependence of the removal rate.

Experimental Section

A detailed description of the experimental setup and procedures is available elsewhere.[9] The apparatus is designed to measure the rate of removal of a solid deposit from the inner surface of a stainless steel pipe under turbulent flow conditions. The calcium phosphate deposits used in this study consisted of either pure DCPD or an HAP/DCPD mixture. The mixture contained a 1:1 weight ratio of HAP and DCPD.

Procedure for Cleaning Experiments. Crystalline aqueous suspensions of HAP (25% solids) and DCPD (25% solids) were obtained from the Sigma Chemical Co. The calcium phosphate deposits were generated from calcium phosphate slurries. DCPD and HAP/DCPD stock slurries were prepared by mixing 8 g of DCPD suspension or 4 g of HAP suspension and 4 g of DCPD suspension, respectively, with 12 g of deionized water. Each of the stock slurries was radio-labeled by the addition of 0.01 mL of ^{32}P-labeled DCPD (approximately 1.5 mg). For each experiment, a volume of 0.5 mL of radio-labeled slurry was injected into the stainless steel test cell, which was a section of pipe with an internal diameter of 1 cm and a length of 4.5 cm. The test cell was then capped and rotated under an infrared heat lamp for 8 h at 95 °C to form a deposit. The temperature was measured from the outside of the cell during deposit preparation. The dry weight of the calcium phosphate deposit is approximately 57 mg.

The test cell was then clamped into the experimental flow system. To noninvasively measure the removal rate of the ^{32}P-labeled deposit, a CaF_2 solid scintillation detector was placed against the outside of the test cell.[9] The detector measured the β emissions from the ^{32}P-labeled deposit on the inner surface of the test cell through a thin stainless steel "window" in the test cell. The data were transmitted by the data acquisition system to a computer every 10 s in units of β-particle counts. These counts represented the amount of radio-labeled deposit remaining on the inner surface of stainless steel tubing as a function of time.

Cleaning solution was pumped through the pipe at fluid velocities ranging from 0.8 to 2.4 m/s within the test cell. These fluid velocities correspond to fully developed turbulent flow in the pipes for *Re* ranging from 9000 to 27 000. The pH was adjusted and main-

tained within ±0.05 pH units by the addition of 0.1 M sulfuric acid or 0.1 M sodium hydroxide throughout the experiment. The counts of the deposit and the pH of the solution were recorded throughout the course of the experiment. Experiments were carried out at room temperature (25 ± 3 °C).

To determine the fraction of deposit remaining on the surface, the data were normalized using the following equation:

$$\frac{M(t)}{M_0} = \frac{C_t(t) - B}{C_{t_0} - B} \tag{28}$$

where $M(t)$ is the mass of deposit on the surface at time t, M_0 is the initial mass of the deposit, $C_t(t)$ is the β-particle count at time t, B is the background count, and C_{t_0} is the initial β-particle count. Background counts were determined by measuring the β-particle count in the absence of a radio-labeled deposit. The normalized data were time averaged over 5 min intervals and plotted as a function of time.

The normalized data represent the fraction of film remaining on the surface, M/M_0. The data were multiplied by the initial mass, M_0, to give the mass of the deposit remaining on the surface as a function of time $M(t)$. A plot of the mass of film remaining on the surface versus time for the initial linear portion of the graph was used to determine the initial removal rates, $dM/dt_{initial}$.

Characterization of the Calcium Phosphate. The composition and morphology of the deposits were examined by SEM. According to the SEM micrographs,[9] the HAP/DCPD deposit consists of threadlike fibers (HAP) and flat rounded platelets (DCPD). The two types of calcium phosphates were uniformly distributed throughout the deposit.

DCPD is a precursor to HAP and may transform into different forms of calcium phosphate upon heating. To verify the identity of the calcium phosphate following heat treatment (95 °C for 8 h), X-ray diffraction analysis (XRD) was carried out on powderized deposits (Diano 8500 wide-angle diffractometer, $\lambda = 0.1542$ nm, nickel-filtered Cu Kα radiation). The XRD patterns showed the strong peaks that are indicative of pure, crystalline material. The peaks matched those of DCPD only.[30] The patterns did not show peaks characteristic of the XRD patterns of other calcium phosphates.[7] No extraneous peaks were found to indicate possible contamination with other solids. Therefore, we conclude that the DCPD deposits are essentially free of impurities and that no transformation of DCPD to other calcium phosphates occurred during the heating process. Similarly, the chemical identity and purity of the HAP/DCPD sample was also confirmed by the XRD patterns. The HAP/DCPD XRD patterns contained strong peaks characteristic of HAP and DCPD only.[30]

To characterize the salts according to the Ca:P ratios, HAP, DCPD, or HAP/DCPD was completely dissolved in hydrochloric acid. Atomic adsorption spectroscopy for calcium and a spectrophotometric method for phosphate were used to determine the total analytical calcium and phosphorus concentrations of the dissolved salts.[31] According to the analysis, pure HAP powder had a Ca:P ratio of 1.63 (as compared to a theoretical value of 1.67 based on stoichiometry). The Ca:P ratio of DCPD was 1.15 (Ca:P (theoretical) = 1.00). For the HAP/DCPD mixture, the Ca:P ratio was 1.41 (versus a calculated value of 1.40 for a 1:1 by weight mixture of HAP and DCPD).

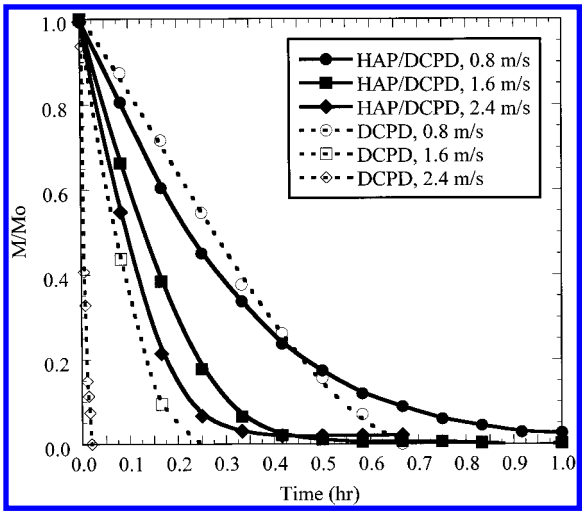

Figure 2. Typical cleaning curves: Removal of HAP/DCPD and DCPD deposits from stainless steel tubing, pH = 2.85. The legend shows the average velocity.

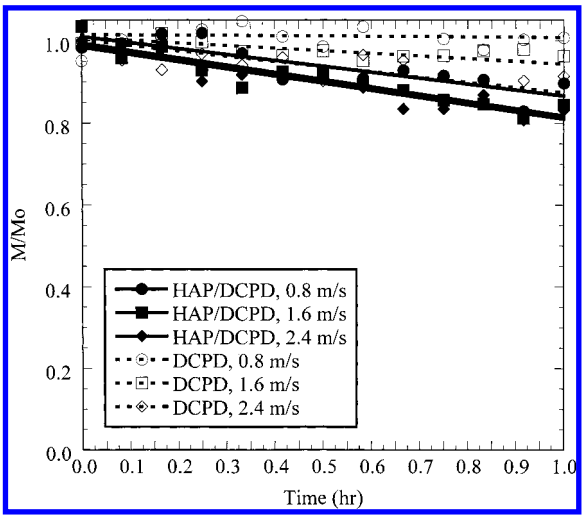

Figure 3. Typical cleaning curves: Removal of HAP/DCPD and DCPD deposits from stainless steel tubing, pH = 5. The legend shows the average velocity.

Results and Discussion

Typical Cleaning Curves. Single-component cleaning studies may be relevant in assessing the influence of HAP and DCPD on the HAP/DCPD mixture. Deposits generated from a slurry consisting only of HAP were inappropriate for cleaning studies, because the deposits washed away immediately upon contact with water. DCPD deposits, on the other hand, remained on the surface following contact with aqueous solutions. Thus, DCPD cleaning studies were conducted. The data were analyzed and compared with the HAP/DCPD cleaning studies.

Typical cleaning curves are shown for pH 2.85 (Figure 2) and pH 5 (Figure 3). The solid and dashed lines indicate HAP/DCPD and DCPD, respectively. As shown in Figure 2, the fluid velocity has a significant effect on the calcium phosphate removal at pH 2.85. A closer inspection reveals that the DCPD cleaning data differ from identical studies carried out with HAP/DCPD. This

finding suggests that the effect of fluid velocity on the removal rate depends on the composition of the deposit.

The upward curvature of the results shown in Figure 2 can be explained in terms of changes of the surface area of the deposit. As cleaning progresses, the amount of material remaining on the surface, M, does not cover the interior of the pipe completely. This results in a decreased total removal rate and, hence, a decrease in the slope of the cleaning curve.

The most obvious difference between the pH 2.85 data (Figure 2) and the pH 5 data (Figure 3) is that the removal rates at pH 5 are dramatically slower. While the deposits are completely removed within an hour at pH 2.85, 80% or more of the calcium phosphate deposits remain on the surface at pH 5 after an hour of cleaning. This result is expected because of the decrease in the calcium phosphate solubility at higher pHs (Figure 1).

Based on the slopes of the cleaning curves in Figure 3, the pH of the solution may also affect the removal mechanism. Both HAP/DCPD and DCPD exhibit a strong velocity dependence at pH 2.85 (Figure 2). While the removal rates of the DCPD deposits continue to show a strong velocity dependence at pH 5, the HAP/DCPD removal rates appear to have a lower velocity dependence (Figure 3).

The data suggest that calcium phosphate removal involves a complex combination of mechanisms. To analyze these trends in greater detail, additional cleaning studies were carried out at various pHs and flow rates. The flux of calcium phosphate from the surface was determined based on initial removal rates measured at the beginning of the experiment (time = 0), because this is the only instance in which we can ensure that the deposit covers the whole pipe surface uniformly. These fluxes were used to ascertain the mechanisms controlling HAP/DCPD and DCPD removal. This is discussed in more depth in the following sections.

Velocity Dependence. As discussed previously, the velocity dependence provides a means of determining the cleaning mechanism according to the following: (i) for processes that are completely interfacial-process-controlled, the removal rate is velocity independent, i.e., v_z^0, (ii) for processes controlled by convective mass transfer, the velocity dependence is $v_z^{0.83}$, and (iii) for shear-controlled removal, the velocity dependence is v_z^2.

To determine the velocity dependence of the experimental data, eq 22 was linearized by the following:

$$\ln(J) = \beta \ln(v_z) + \ln(\kappa) \tag{29}$$

where β is a constant. The flux J was calculated according to the following definition:

$$J = -\frac{1}{M_w S}\left(\frac{dM}{dt}\right)_{initial} \tag{30}$$

The initial removal rate, $(dM/dt)_{initial}$ was determined from experimental cleaning data as described previously in the experimental methods. The surface area of the deposit, S, was assumed to be constant. For the HAP/DCPD deposits, the molecular weight, M_w, was calculated based on a 1:1 weight ratio of HAP and DCPD.

A plot of $\ln(J)$ versus $\ln(v_z)$ for the HAP/DCPD cleaning studies is shown in Figure 4. The fluid velocities shown range from 0.8 to 2.4 m/s. The slopes of the lines are the velocity exponent β. The effect of fluid velocity on the removal rate is difficult to discern at pH 10 because of extremely slow removal rates (4×10^{-4} mg/s on average) and a large amount of scatter.

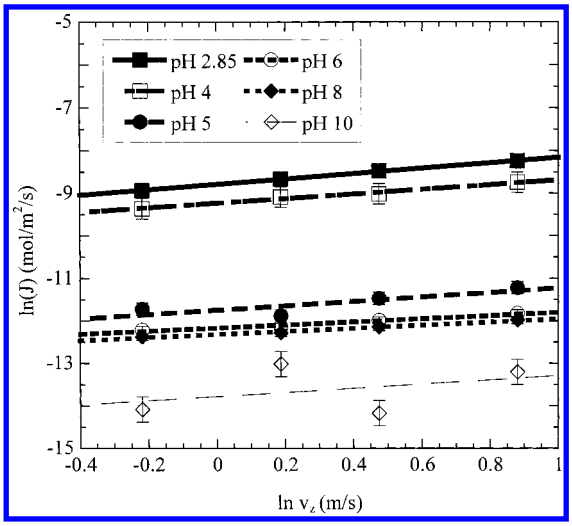

Figure 4. Velocity dependence of HAP/DCPD removal. The lines represent best fits of the data according to eq 29.

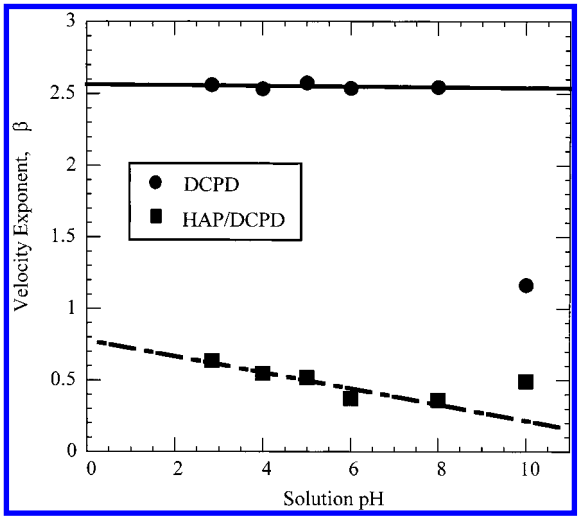

Figure 5. Velocity exponent for HAP/DCPD and DCPD removal. The lines represent best fits of the data excluding the pH = 10 data (as discussed in the text).

From Figure 4, the velocity exponents were obtained as functions of the solution pH for HAP/DCPD removal. A similar procedure was followed for pure DCPD deposits. The results are shown in Figure 5. Note that, because of difficulties associated with determining the effect of flow rate on calcium phosphate removal at pH 10, the velocity exponent cannot be accurately determined. Thus, the pH 10 data presented in Figure 5 are not included in the analysis of the velocity dependence.

The HAP/DCPD deposits have velocity exponents that are always lower than 0.83. This means that, over the range of pHs explored, the removal is controlled by a combination of interfacial dissolution and mass transfer. As the pH decreases, the increased solubility of the deposits makes the interfacial dissolution rate faster, and the exponent increases to reflect an enhanced mass-transfer role. It is interesting to point out that an extrapolation of the exponent to very low pHs shows a trend of the exponent to approach 0.8, which would indicate complete mass-transfer control and very fast interfacial dissolution. The fact that this would occur

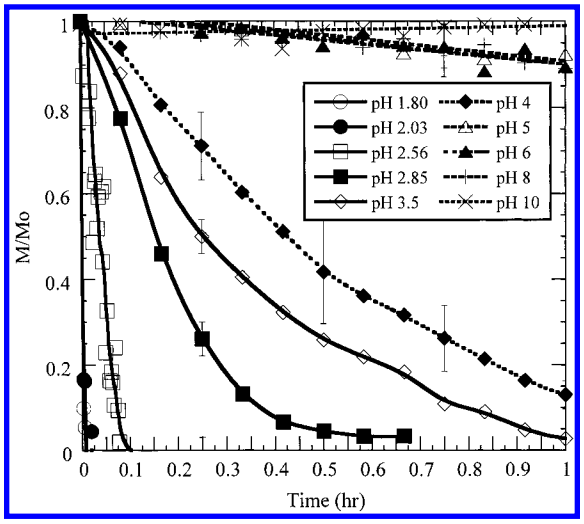

Figure 6. Removal of HAP/DCPD deposits from stainless steel for various pHs (average velocity: 1.2 m/s).

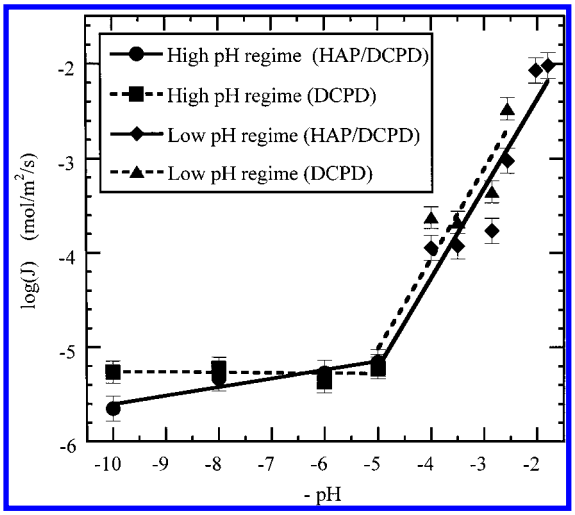

Figure 7. pH dependence of HAP/DCPD and DCPD removal.

only at unrealistically low pH values underlines the importance of considering interfacial kinetics in practice.

The DCPD deposits exhibit a completely different trend; the velocity exponent is approximately 2.6 for all pHs (Figure 5). Such a high exponent would be consistent only with removal by shear forces. The fact that the mechanism does not change with pH indicates that shear removal accounts for removal to a greater magnitude than dissolution and mass transfer, even at low pHs. As stated previously, the shear stress is proportional to the square of the average velocity. However, the actual force exerted on particles protruding from the film might show a more pronounced velocity variation, which would be consistent with the high exponent obtained here. For example, Cleaver and Yates[33] present an analysis of colloidal particle detachment in turbulent flows, which indicates that particles are subjected to a lift force that is proportional to the cubic power of the average velocity. This lift force is a consequence of localized turbulence bursts occurring next to the wall on which the particle is attached.

The fact that HAP/DCPD and DCPD deposits are cleaned by completely different mechanisms suggests that the behavior of complex calcium mineral deposits may not be accurately established from simplified studies of the individual components.

pH Dependence. As shown in Figure 6, the removal rates of HAP/DCPD deposits are clearly a function of pH. Similar variations were obtained for DCPD deposits. We base our analysis on the postulate that the pH dependence for mineral dissolution in the presence of a strong acid can be expressed as follows:

$$J = k_1' = k_1[\mathrm{H}^+]^n \qquad (31)$$

In this equation, $[H^+]$ represents the concentration of protons at the interface. We will assume that transport of protons is fast, so that the interfacial proton concentration is also the bulk concentration as given by the pH.[10,13] In view of the fact that mass transfer of products from the interface to the bulk is not the slow step in the removal process (as demonstrated by Figure 5), we have neglected the rate of the backward reaction in eq 13. Essentially, this means that there is always appreciable undersaturation at the interface, $[Ca^{2+}]_i/[Ca^{2+}]_s \ll 1$; see eq 18. According to eq 31, the exponent representing proton dependence n is determined from the slope of a plot of log J versus $-$pH (or log $[H^+]$).

As shown in Figure 7, two pH regimes exist for HAP/DCPD and for DCPD removal. At the low pHs, the removal rate is significantly influenced by the pH. For pHs < 5, a first-order dependence on the hydrogen ion concentration was measured for both HAP/DCPD and DCPD. For the case of HAP/DCPD removal, this result indicates that the interfacial dissolution occurs by proton attack of the solid surface, i.e., a net reaction analogous to eq 16. At high pHs, the rate is approximately independent of pH. This result is indicative of a dissolution reaction that is controlled by a process involving H_2O rather than a proton source, i.e., a net reaction analogous to eq 14.

The removal rate of pure DCPD follows approximately the same trends with pH as the HAP/DCPD deposits. This might seem surprising at first, because the removal mechanisms are completely different. However, the shear removal of DCPD depends not only on the shear stress that needs to be exerted to detach solid particles from the film, τ_w, but also on the intrinsic stress that needs to be overcome for detachment, τ_c. Our contention is that the interfacial dissolution reaction, which depends on pH, softens the solid deposit, thereby changing the value of τ_c accordingly. We then find that, under acidic conditions (pH < 5), the shear removal rate increases as the pH decreases because the shear stress can detach solid particles faster as local dissolution rates erode the solid film.

The fact that the transition between pH regimes occurs at about pH 5 is interesting. According to the solubility diagram for DCPD (Figure 1), the solubility of DCPD is minimal at a pH of approximately 8. Nevertheless, batch DCPD dissolution studies seem to denote a somewhat related trend. Zhang and Nancollas[21] observed an unexpected minimum in the DCPD dissolution rate at about pH 5 for a relative undersaturation of 0.5. It was suggested that this minimum occurred at the transition of the DCPD dissolution mechanism from a regime based on proton catalysis to a regime characterized largely by stoichiometric ionic fluxes. While our cleaning rates are pH independent for pHs above 5 (Figure 7), the aforementioned change in the pH dependence is indicative of a change in the dissolution process.

The surface chemistry of hydroxyapatite dissolution

is complex. The Ca:P ratio of hydroxyapatite equilibrated in aqueous media was found to approach the limiting value of 1.67, but during the dissolution of hydroxyapatite in aqueous media, the dissolution of hydroxyapatite was nonstoichiometric.[33] The incongruent (i.e., nonstoichiometric) dissolution process is attributed to ion adsorption, the sequential release of calcium followed by phosphate, and the formation and/or precipitation of calcium phosphate intermediates, such as DCPD, OCP, and ACP, during the dissolution process.[34] The pH dependence for HAP/DCPD removal measured in this work (i.e., $n = 1$ for low pHs and $n = 0$ for high pHs) may be due to the dissolution kinetics of HAP or DCPD or a combination of both species.

The pH dependence for HAP/DCPD removal from tubing differs from batch dissolution studies carried out with HAP and human enamel powder. Christoffersen et al.[10] observed $n = 0.57$ for pHs ranging from 6.6 to 7.2 for HAP dissolution, while Thomann et al.[14] reported $n = 0.64$ for human enamel powder for pHs ranging from 3.7 to 6.9. According to Thomann et al., this pH dependence was different from the $n = 0.81$ dependence reported for HAP dissolution under similar conditions. A number of differences in the experimental techniques, flow patterns, and material studied may account for the differences between the pH dependence of the HAP/DCPD cleaning studies and those of the dissolution studies reported previously.

Conclusions

The analysis shows that the removal mechanisms for calcium phosphate deposits vary depending on the deposit composition and the solution pH. Interfacial kinetics controls the HAP/DCPD removal process, particularly at high pHs. As the pH decreases, the removal mechanism approaches a mass-transfer-limited process. Therefore, the removal of HAP/DCPD deposits occurs because of a combination of rate-limiting processes, and the mechanism varies depending upon the cleaning conditions. In contrast, the removal of DCPD exhibited a strong velocity dependence over the wide range of pHs. The comparison of the experimental data to the limiting cases indicates that the removal rate is controlled by fluid shear. Overall, the rate-controlling mechanism of HAP/DCPD removal does not appear to be directly related to the results of single-component cleaning studies.

The interfacial process involved in the dissolution process was found to be the kinetics of the dissolution reaction taking place on the crystal surface. The pH dependence showed that two pH regimes exist: a low pH regime (pH < 5) and a high pH regime (pH > 5). Within the low pH regime, the dissolution process was first order with respect to the proton concentration. In the high pH regime, the dissolution process was essentially pH independent. This work will provide a foundation for future work in the study of novel cleaning agents.

Acknowledgment

We gratefully acknowledge support by the National Science Foundation (Grants CTS-9500399 and CTS-9616638). We also thank Dr. Ruben Carbonell for input in the development of the theory. We also acknowledge the Nuclear Engineering Department at North Carolina State University (Pedro Perez, Jack Weaver, and Jerry Wicks) for supplying the radio-labeled calcium phosphate for the solid scintillation cleaning studies and Dr. Matthew Tirrell for use of the SEM facilities at the NSF Center for Interfacial Engineering at the University of Minnesota. Also, we acknowledge the contributions of Kit Yeung and Brad Rudiger.

Nomenclature

A = temperature-dependent constant in the Davies expression (eq 10)
a_j = activity of species j
a, b, c = parameters defined in the Gilliland and Sherwood correlation
B = β-particle background count
C_b = bulk concentration of calcium phosphate
C_i = concentration of species at the interface
C_s = concentration of species at saturation
C_t = β-particle count at time t
C_{t_0} = β-particle count at time zero
D = diameter of the fluid cross section
D_A = diffusivity of the dissolving species
f = Darcy friction factor
h = fraction of the surface occupied by HAP
I = ionic strength
J = molar flux
J_D = molar flux of calcium ions from DCPD
J_H = molar flux of calcium ions from HAP
J_{HD} = molar flux of calcium ions from a HAP/DCPD mixture
k_1' = apparent forward rate constant
k_{-1} = reverse rate constant
k_{dcpd} = solubility product constant for DCPD
k_{hap} = solubility product constant for HAP
K_{Eq} = ion solubility product of DCPD corrected with activity coefficients
k_m = mass-transfer coefficient
L = length of the mass-transfer region
M = mass of the calcium phosphate deposit
M_0 = initial mass of the calcium phosphate deposit
M_w = average molecular weight of the film
Re = Reynolds number = $\rho v D/\mu$
Sc = Schmidt number = $\mu/\rho D_A$
Sh = Sherwood number = $k_m D/D_A$
t = time
v_z = average velocity of the bulk solution
z = axial distance
z_j = valence of species j

Greek Letters

α = molar ratio of $[HPO_4^{2-}]$ to [P]
β = velocity dependence from a generalized correlation (eq 22)
β_D = velocity dependence for DCPD
β_H = velocity dependence for HAP
β_{HD} = velocity dependence for a HAP/DCPD mixture
γ_j = activity coefficient of species j
μ = viscosity of the bulk fluid
ρ = density of the bulk fluid
τ_c = force per unit area that the agglomerated crystals can withstand intact
τ_w = shear stress exerted at the solid/liquid interface

Literature Cited

(1) Amjad, Z. Effect of Precipitation Inhibitors on Calcium Phosphate Scale Formation. *Can. J. Chem.* **1989**, *67*, 850.

(2) Irving-Monshaw, S. Nonchromates Vie for a Cooling Water Niche. *Chem. Eng.* **1989**, *96*, 59.

(3) Sandu, C.; Lund, D. Fouling of Heating Surfaces—Chemical Reaction Fouling Due to Milk. In *Fouling and Cleaning in Food*

Processing Proceedings; Lund, D., Plett, E., Sandu, C., Eds.; University of Wisconsin—Madison Extension: Madison, WI, 1985.

(4) Gaffar, A.; LeGeros, R. Z.; Gambogi, R. J.; Afflitto, J. Inhibition of Formation of Calcium Phosphate Deposits on Teeth and Dental Materials: Recent Advances. *Adv. Dent. Res.* **1995**, *9*, 419.

(5) Corbridge, D. E. C. *The Structural Chemistry of Phosphorus*; Elsevier Scientific: New York, 1974.

(6) Brown, W. E. Solubilities of Phosphates and Other Sparingly Soluble Compounds. In *Environmental Phosphorus Handbook*; Griffith, E. J., Beeton, A., Spencer, J. M., Mitchell, D. T., Eds.; John Wiley and Sons: New York, 1973.

(7) Elliott, J. C. *Structure and Chemistry of the Apatites and Other Calcium Orthophosphates*; Elsevier: New York, 1994.

(8) Grant, C. S.; Webb, G. E.; Jeon, Y. W. Calcium Phosphate Decontamination of Stainless Steel Surfaces. *AIChE J.* **1996**, *42*, 861.

(9) Littlejohn, F.; Sáez, A. E.; Grant, C. S. The Use of Sodium Polyaspartate in the Removal of Hydroxyapatite/Brushite Deposits from Stainless Steel Tubing. *Ind. Eng. Chem. Res.* **1998**, *37*, 2691.

(10) Christoffersen, J.; Christoffersen, M. R.; Kjaergaard, N. The Kinetics of Dissolution of Calcium Hydroxyapatite in Water at Constant pH. *J. Cryst. Growth* **1978**, *43*, 501.

(11) Christoffersen, J.; Christoffersen, M. R. The Kinetics of Dissolution of Calcium Hydroxyapatite. II. Dissolution in Non-Stoichiometric Solutions at Constant pH. *J. Cryst. Growth* **1979**, *47*, 671.

(12) Christoffersen, J.; Christoffersen, M. R. The Kinetics of Dissolution of Calcium Hydroxyapatite. III. Nucleation-controlled Dissolution of a Polydisperse Sample of Crystals. *J. Cryst. Growth* **1980**, *49*, 29.

(13) Thomann, J. M.; Voegel, J. C.; Gramain, Ph. Kinetics of Dissolution of Calcium Hydroxyapatite Powder. II: A Model Based on the Formation of a Self-Inhibiting Surface Layer. *J. Colloid Interface Sci.* **1989**, *132*, 403.

(14) Thomann, J. M.; Voegel, J. C.; Gramain, Ph. Kinetics of Dissolution of Calcium Hydroxyapatite Powder. III: pH and Sample Conditioning Effects. *Calcif. Tissue Int.* **1990**, *46*, 121.

(15) Thomann, J. M.; Voegel, J. C.; Gramain, Ph. Kinetics of Dissolution of Calcium Hydroxyapatite Powder. IV. Interfacial Calcium Diffusion Controlled Process. *Colloids Surf.* **1991**, *54*, 145.

(16) Thomann, J. M.; Voegel, J. C.; Gramain, Ph. Kinetics of Dissolution of Calcium Hydroxyapatite with a Permselective Ionic Interface. *J. Colloid Interface Sci.* **1993**, *157*, 369.

(17) Christoffersen, M. R.; Christoffersen, J. The Kinetics of Crystal Growth and Dissolution of Calcium Monohydrogen Phosphate Dihydrate. *J. Cryst. Growth* **1988**, *87*, 51.

(18) Nancollas, G. H.; Marshall, R. W. Kinetics of Dissolution of Dicalcium Phosphate Dihydrate Crystals. *J. Dent. Res.* **1971**, *50*, 1269.

(19) Zhang, J.; Nancollas, G. H. Dissolution Deceleration of Calcium Phosphate Crystals at Constant Undersaturation. *J. Cryst. Growth* **1992**, *123*, 59.

(20) Zhang, J.; Nancollas, G. H. Interpretation of the Dissolution Kinetics of Dicalcium Phosphate Dihydrate. *J. Cryst. Growth* **1992**, *125*, 251.

(21) Zhang, J.; Nancollas, G. H. Unexpected pH Dependence of Dissolution Kinetics of Dicalcium Phosphate Dihydrate. *J. Phys. Chem.* **1994**, *98*, 1689.

(22) Compton, R. G.; Brown, C. A. Monitoring Particle Sizes with Rotating Disc Electrodes: Measurement of the Dissolution Kinetics of Calcite. *J. Colloid Interface Sci.* **1993**, *158*, 243.

(23) Fredd, C. N.; Fogler, H. S. The Kinetics of Calcite Dissolution in Acetic Acid Solutions. *Chem. Eng. Sci.* **1998**, *53*, 3863.

(24) Wu, M.; Higuchi, W. I.; Fox, J. L.; Friedman, M. Kinetics and Mechanism of Hydroxyapatite Crystal Dissolution in Weak Acid Buffers Using the Rotating Disk Method. *J. Dent. Res.* **1976**, *55*, 496.

(25) Compton, R. G.; Pritchard, K. L.; Unwin, P. R.; Grigg, G.; Silvester, P.; Lees, M.; House, W. A. The Effect of Carboxylic Acids on the Dissolution of Calcite in Aqueous Solutions. Part I. Maleic and Fumaric Acids. *J. Chem. Soc., Faraday Trans.* **1989**, *85*, 4335.

(26) Welty, J. R.; Wicks, C. E.; Wilson, R. E. *Fundamentals of Momentum, Heat, and Mass Transfer;* Wiley: New York, 1984.

(27) Gregory, T. M.; McDowell, H.; Brown, W. E. Solubility of $CaHPO_4 \cdot 2H_2O$ in the System $Ca(OH)_2-H_3PO_4-H_2O$ at 5, 15, 25, and 37.5 °C. *J. Res. Natl. Bur. Stand., Sect. A* **1970**, *74A*, 461.

(28) McDowell, H.; Gregory, T. M.; Brown, W. E. Solubility of $Ca_5(PO_4)_3OH$ in the System $Ca(OH)_2-H_3PO_4-H_2O$ at 5, 15, 25, and 37 °C. *J. Res. Natl. Bur. Stand., Sect. A* **1977**, *81A*, 273.

(29) Davies, C. W. *Ion Association*; Butterworth: London, 1962.

(30) Berry, L. G., Ed. *Selected Powder Diffraction Data for Minerals—Data Book*; Joint Committee on Powder Diffraction Standards: Swarthmore, 1974.

(31) Murphy, J.; Riley, J. P. A Modified Single Solution Method for the Determination of Phosphate in Natural Waters. *Anal. Chim. Acta* **1962**, *27*, 31.

(32) Lund, K.; Fogler, H. S.; McCune, C. C.; Ault, J. W. Acidization II. The Dissolution of Calcite in Hydrochloric Acid. *Chem. Eng. Sci.* **1975**, *30*, 825.

(33) Cleaver, J. W.; Yates, B. Mechanism of Detachment of Colloidal Particles from a Flat Substrate in Turbulent Flow. *J. Colloid Interface Sci.* **1973**, *44*, 464.

(34) Mika, H.; Bell, L. C.; Kruger, B. J. The Role of Surface Reactions in the Dissolution of Stoichiometric Hydroxyapatite. *Arch. Oral Biol.* **1976**, *21*, 697.

Received for review August 18, 1999
Revised manuscript received January 6, 2000
Accepted January 12, 2000

IE990624H